View metadata, citation and similar papers at core.ac.uk

brought to you by CORE

provided by DSpace@MIT

PSFC/JA-05-49

Startup characteristics of plasmatron gasoline reformers

L. Bromberg

December 15, 2005

MIT Plasma Science and Fusion Center

Work supported by the US Department of Energy, Office of FreedomCar and Vehicle Technologies

Abstract

The startup characteristics of plasmatron reformers with gasoline fuel for the generation of hydrogen rich gas is discussed. A brief set of experiments has been carried out at a single fuel and air flow rate. The air/fuel mixture preparation, especially the implications of the gasoline vaporization, has been modeled using a CFD code.

I. Introduction

We have previously reported in a series of papers [1-6] the performance of a plasmatron reformer using methane and propane. That work provides increased understanding of the behavior of the plasmatron reformer operating with heavier hydrocarbons. In a previous paper the homogeneous reformation of refined and unrefined vegetable oils and ethanol have been reported [7]. In this paper the results of plasmatron gasoline reformer operation during startup are discussed..

The performance of liquid fuels and gaseous fuels is very different due to the latent heat of vaporization of the liquid fuel. In reference 7 we reported exclusively in the steady state characterization of the plasmatron. There are three main differences between liquid and gaseous fuels. First, there is a finite rate of vaporization of the fuel, and thus either combustion occurs as a diffusion flame (as is the case in a diesel engine). The second has to do with the heat of vaporization of the fuel, which cools the air/fuel mixture. Finally, because of the need to prevent wall coating, the liquid fuel is exclusively injected through the axial port, while the gaseous fuels could be injected through any set of ports, and indeed had best performance when injected through the swirl gas.

Section II discusses the setup and the characteristics of the plasmatron gasoline reformers, in particular the effect of the fuel atomization and the cooling of the air/fuel mixture due to the latent heat of vaporization of the gasoline. Section III describes a simple CFD model that is useful to understand the air/fuel mixing, as well as the vaporization of the gasoline droplets. Section IV describes the experimental results for gasoline transients. Section V summarizes the work.

II. Experimental setup

The experimental setup has been described in [1] and will only be briefly described here. The plasmatron used is the same used in [1-7] and is shown in Figure 1.

The experiments reported in [1-6] were carried out with gaseous fuels, and there was no need for an additional pump for the liquid fuel or for liquid fuel atomization. For liquid fuels, the approach used in the plasmatron fuel reformer work has been to form a fine spray from the liquid fuel, followed by air assist atomization. We expect to have droplet size on the order of $< 20\ \mu m$. The liquid fuels in the present tests have been introduced into the plasmatron through a nozzle that forms a fine spray of droplets. The nozzle used in these experiments is a B-37 nozzle. The characteristics of this nozzle are given in Reference [7].

The atomization air flow rate was monitored by a TSI air flow sensor. The TSI sensor was also used to confirm that the two other mass-flow controllers (for the wall air and for the plasma air) were within certification.

The fuel pump used to pressurize and monitor the flow rate was a variable displacement pump attached to a variable speed drive from Fluid Metering. The pump was calibrated

by capturing and then weighing the fluid for a given amount of time. The adjusted parameter was the speed of the drive. The pump provides constant flow rate for pressures lower than about 200 psi, and we have stayed below this limit, operating close to 50 psi.

Figure 1. Photograph of the plasmatron used in these experiments, as well as those in reference [1-7].

The transient gas analysis was determined using an electrostatic quadrupole mass spectrometer, from Pfeiffer. The mass spectrometer setup was described in [2]. The Soot/raw fuel droplets were measured using a Wagner 2000 opacity meter.

Conventional 87 octane gasoline was used in the experiments.

III. CFD Modeling in the absence of chemistry

The calculations were performed using FLUENT 6.0 CFD package. The solution is for a steady state solution, axisymmetric, with air as the fluid. A Reynolds-Average Navier-Stokes model has been chose, with a k-ε formulation for the turbulence. The model includes swirl and compressibility of the air. The energy equation is solved. The solution is shown on half of the cross section of the plasmatron. A small section (1 in) long of the reaction extension cylinder is also included in the model.

No chemistry is assumed. Wall temperatures are at the same temperature as the gas (300K). The outlet condition is atmospheric pressure. Inlet conditions in all three ports (plasma air, wall air, atomization air) are as mass flow rate. Under-relaxation has been

used for the pressure (0.3) and momentum (0.7). The scheme for solution is 2nd order upwind.

Table 1 shows the parameters used in the calculations. The gasoline flow rate assumed was 1 g/s, twice that of the experiments. The fuel was injected using "surface" injection at the port for the atomization air (uniformly distributed). Fuel droplets were injected exclusively in the axial direction, with no radial or tangential component, that is, with a zero spray angle. It was assumed that the injection velocity of the droplets was 50 m/s. The droplets composition was n-octane and uniform in diameter, with the droplet size in the first set of calculations is assumed to be 50 μm. This is a relatively large drop size. Evaporation of the droplets was included, and the concentrations of the n-octane vapors have been calculated. Smaller drop sizes will be considered later in this paper. Finally, the effects of spray distribution are discussed in the last section.

A. 50 μm diameter droplets

In this section, the upper range of the particulate size is investigated.

Table 1
Plasmatron gen 3A

Plasma air	0.0018 g/s	
Velocities: swirl	50./s	
Radial	-12 m/s	
Wall air	0.0028 g/s	
Atomization air	0.0013 g/s	
Atomization air temp	300 K	
Fuel injection		
Droplet size	50 μm	
Initial droplet speed	-50 m/s	
Composition of droplet	n-octane liquid	
Spray angle	0	

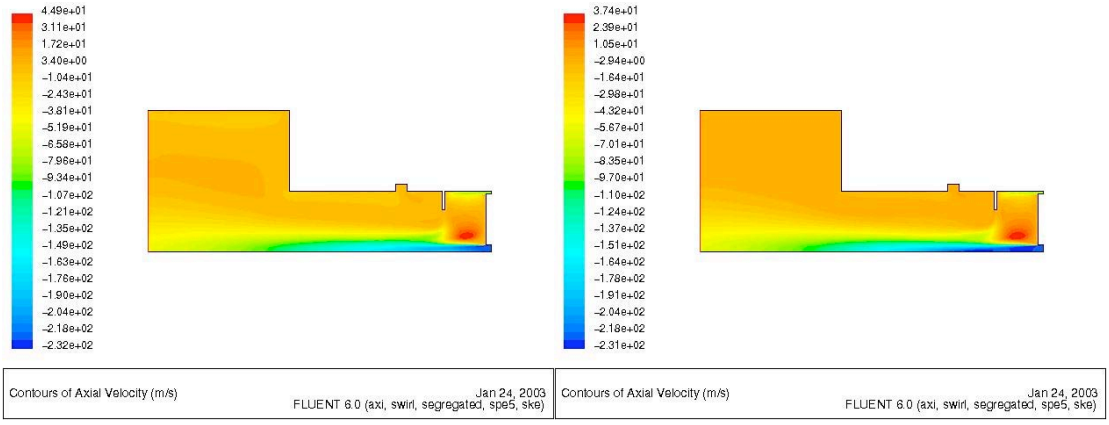

Figure 2. Axial velocity of the gas (a) with fuel injection (1 g/s) (b) no fuel injection

Figure 2 shows the axial velocity of the gas in the plasmatron for the conditions of Table 1, with and without fuel. Note that the axial velocity of the atomization air is lower in the case of the fuel injection than without, reflecting the fact that momentum is being transferred from the gas to the droplets, which are injected with lower speed (50 m/s).

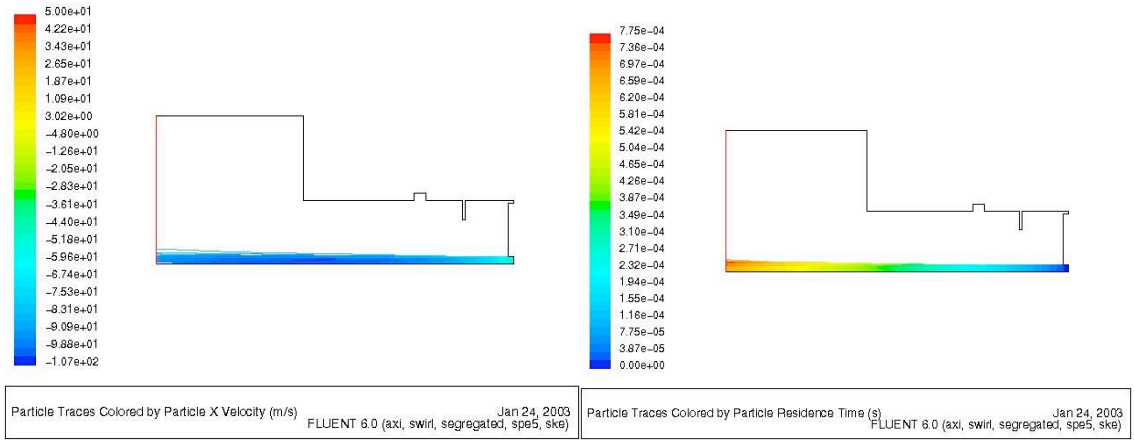

Figure 3. Droplet average path (a) droplet axial velocity (b) droplet residence time

Figure 3 shows results of calculations of n-octane droplets. The calculations are performed using stochastic air and droplet flow fields, with multiple droplets launched at the surface of the nozzle. Figure 3a shows the calculated droplet velocity on the droplet path, while Figure 3b shows the residence time. The droplets quickly achieve the velocity of the gas (air), by the time that they reach the interlectrode spacing they are well entrained in the atomization air flow.

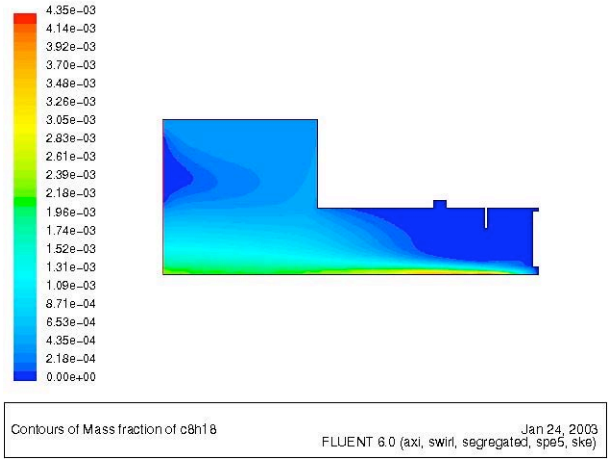

Figure 4. Mass fraction of Gaseous C8H18 (relative to nitrogen)

The mass concentration of gaseous n-octane is shown in Figure 4 for the case of 50 mm droplets. Only a small fraction of the fuel has vaporized, and the conditions for stoichiometric conditions (about 6% by mass for an air/fuel ratio of 15) are not reached with the fuel vapor.

B. 10 μm diameter droplets

In order to examine the other extreme of the droplet size distribution, the calculations were performed with 10 mm diameter droplets. The smaller droplets size results in increased evaporation of the droplets, due to increased surface area, as well as in reduced particulate inertia, with increased impact on the droplet paths due to the turbulence of the gas.

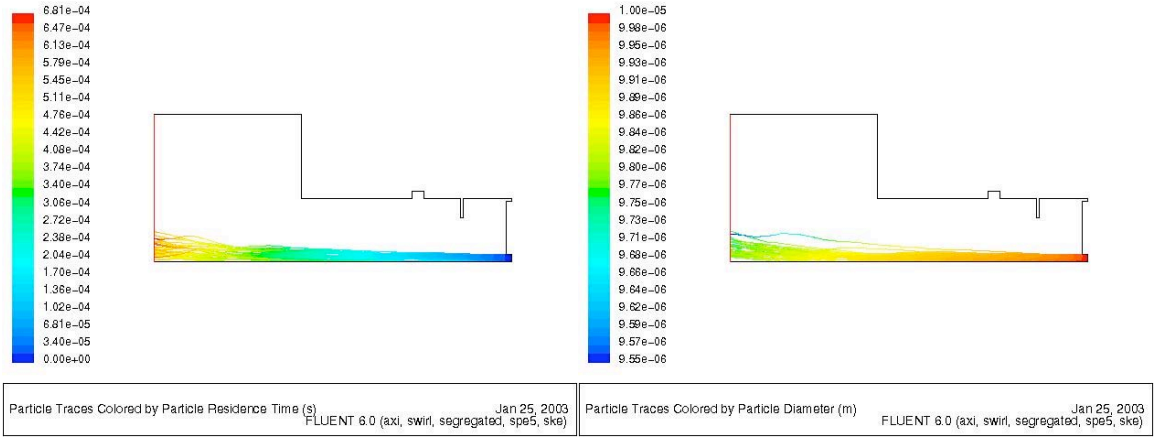

Figure 5. Stochastic particle path vs (a) residence time (b) particle diameter

The random paths of some droplets, launched at different locations on the nozzle surface, are shown in Figure 5. Different sets of droplets have been used in Figures 5 (a) and (b), as noticed by the outermost droplets. Figure 5a shows the residence times of the particulates, while Figure 5b shows the droplet diameter. Some evaporation of the particle is seen, more than in the case with 50 mm particles. However, even at the inter-electrode location (where the plasma is expected), the droplet diameter has decreased by only about 1%, corresponding to about 3% of the droplet. The corresponding concentration of n-octane is shown in Figure 6.:

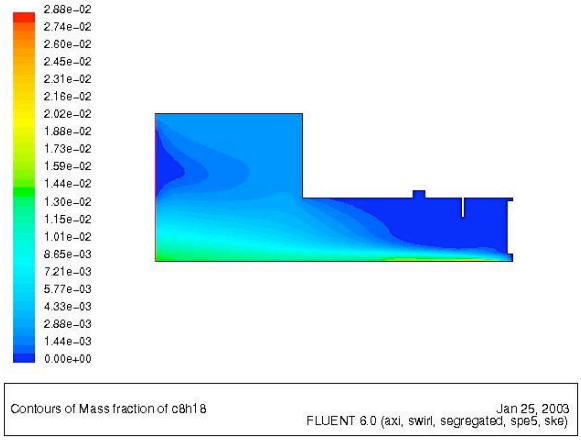

Figure 6. Concentration (by mass) of gaseous n-octane

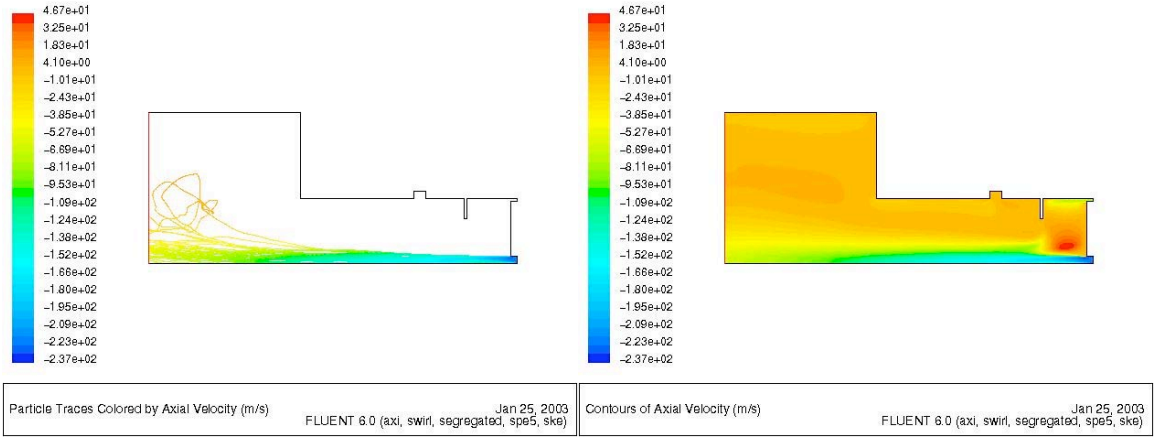

Figure 7. Axial velocity (a) of droplets along their path (b) of continuous media

As expected, with the smaller particle size there is stronger interaction between the continuous media and the droplets. Thus, in the case with smaller droplet size the atomization air slows down quicker and the droplets gain speed faster than in the case with larger droplet size. Also, the path of the smaller droplets (stochastically calculated in every plot) is influenced more by the local turbulence of the flow.

C. Finite spray angle

The surface injection has no capability of spray angle distribution, but it can have a non-zero radial speed (with no spread, therefore resulting in a cone-shape). Since the effect is more pronounced with the smaller droplets, the calculations of the effect of finite spray angle has been performed for 10 μm droplets.

The initial radial speed of the droplets was varied from 0 through 30 m/s. The initial axial speed of the droplets was kept constant at 50 m/s. Therefore, relatively wide spray angles were modeled.

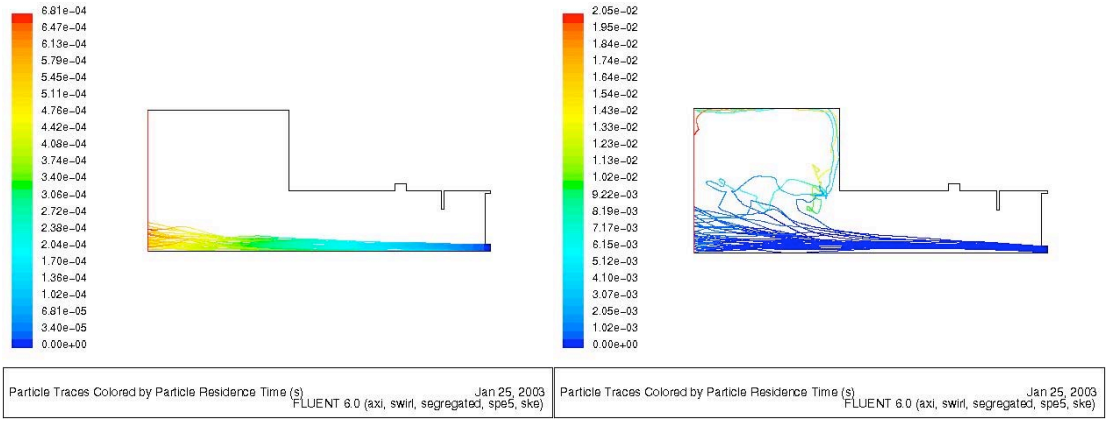

Figure 8. Stochastic paths for initial radial velocities of (a) 0 m/s, and (b) 10 m/s

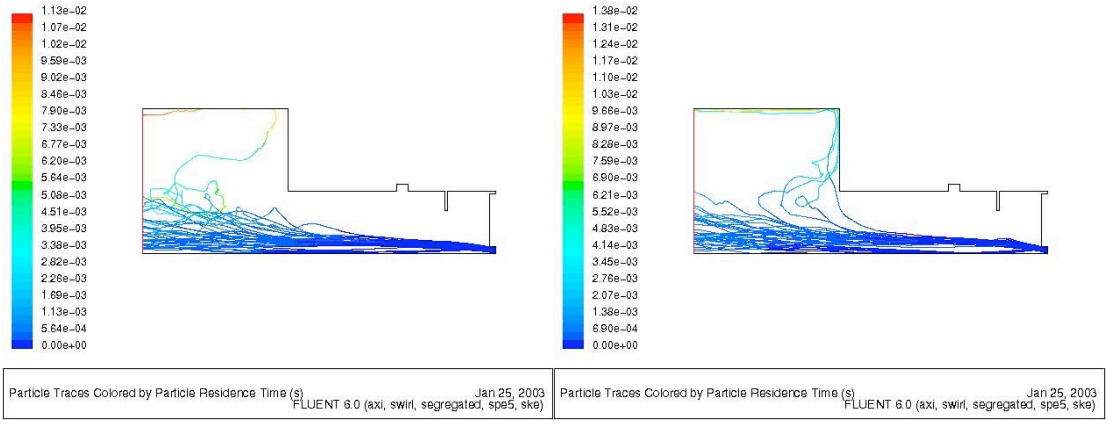

Figure 9. Stochastic paths for initial radial velocities of (a) 20 m/s, and (b) 30 m/s

The radius of the droplet "cloud" increases slightly when the initial radial speed of the droplets increases from 0 to 10 m/s. However, the location of the paths in the inter-electrode region do not change substantially when the initial radial velocity of the droplets increases further from 10 through 30 m/s

The complex vaporization process made modeling of the system very difficult, and it has been analyzed in a simplified CFD model. The simple models of the plasmatron, without chemistry, show that indeed very small fraction of the gasoline is vaporized.

D. Cooling of the gas by evaporating fuel

The gasoline droplets need some heat in order to vaporize. The vaporization rate of the droplets follows the rule

$$dD^2/dt = -K_e$$

Where K_e is the evaporation constant and is a function of temperature. For stoichiometric combustion, the change in the temperature of the air due to the vaporization of the gasoline is about 24 K, assuming constant pressure process. However, for partial oxidation, where the air/fuel mass ratio is about 1/3 that of stoichiometric combustion, the temperature of the air is reduced by as much as 70 K (assuming constant thermodynamic properties of the air). These large drop in temperature means that only a small fraction of the gasoline will be vaporized prior to entering the reaction zone, where exothermic reactions raise the temperature of the gas.

V. Transient experiments with gasoline

The plasmatron setup described in section II was used to determine the startup characteristics of the plasmatron. Only one set of experiments was carried out, at an O/C ratio of the experiments is 1.06, near ideal partial oxidation, and at a power of 300 W.

The measured hydrogen concentration is shown in Figure 10. The experiments were carried out by turning on the air flow, the plasma, and then the fuel.

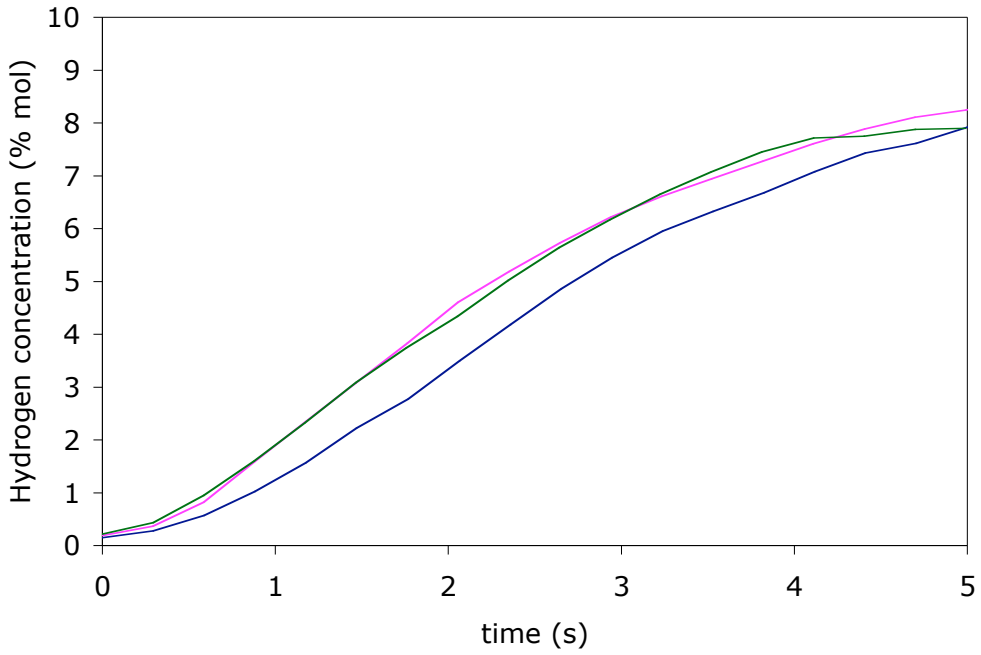

Figure 10. Measured concentration of H_2 as a function of time, for 3 startups.

After the early startup, the hydrogen concentration drops to ~ 4 %. It is likely that his process occurs because of changes in the air/fuel mixture characteristics. After a few seconds, the hydrogen concentration starts to increase rapidly.

The soot concentration, as measured with the opacity meter, was below measurable values.

VI. Summary

Experiments and modeling of the vaporization with the time response of a plasmatron gasoline reformer were carried out.

We have determined that the response time of the mass spectrometer is on the order of 1 s. Thus, it is likely that the hydrogen concentration reaches about 4% 1 s after turn-on. By comparison, the response time with gaseous fuels was on the order of 2 s, at substantially higher O-to-C ratios..

Acknowledgement

We want to thank the continued support of Dr. Sidney Diamond. His encouragement, depth and width of knowledge, enthusiasm and *`Joye de Vivre'* will serve as standards for us to emulate. Dr. Kamal Hadid helped to operate the mass spectrometer during the experiments.

References

[1] L. Bromberg, K. Hadidi and D.R. Cohn, *Experimental Investigation of Plasma Assisted Reforming of Methane I: Steady State Operation,* Plasma Science and Fusion Center Report JA-05-10

[2] L. Bromberg, K. Hadidi and D.R. Cohn, *Experimental Investigation of Plasma Assisted Reforming of Methane II: Start-up,* Plasma Science and Fusion Center Report JA-05-11

[3] L. Bromberg and N. Alexeev, *Plasma Assisted Reforming of Methane: Two Stage Perfectly Stirred Reactor (PSR) Simulation*, Plasma Science and Fusion Center Report JA-05-12

[4] L. Bromberg, *Modeling of Plasma Assisted Reforming of Methane II: Partially Stirred Reactor (PASR) Simulation*, Plasma Science and Fusion Center Report JA-05-13

[5] L. Bromberg, *CFD modeling of Plasmatron Methane Reformers*, Plasma Science and Fusion Center Report JA-05-14

[6] L. Bromberg, K. Hadidi and D.R. Cohn, *Experimental Investigation of Plasma Assisted Reforming of Propane,* Plasma Science and Fusion Center Report JA-05-15

[7] L. Bromberg, K. Hadidi, D.R. Cohn, *Plasmatron Reformation of Renewable Fuels*, Plasma Science and Fusion Center Report JA-05-3